SPECTROSCOPIC STUDY OF SECOND-ORDER RAMAN SCATTERING AND DETERMINATION OF THE TWO-PHONON STATE DENSITY EXTREMES IN ZnO CRYSTALS

V.O. GUBANOV, N.I. BEREZOVSKA

Taras Shevchenko Kyiv National University, Faculty of Physics
(6, Academician Glushkov Prosp., Kyiv 03127, Ukraine; e-mail: n_ berezovska@univ.kiev.ua)

UDC 543.424

The polarized second-order Raman spectra of ZnO crystals have been studied and interpreted on the basis of the group-theoretic analysis of selection rules and critical points in the phonon dispersion which had been obtained using the mathematical apparatus of projective representations. The Γ, A, M, L, K, H, Δ, Σ, and T points of the Brillouin zone have been studied. The trend of the phonon dispersion curve in the $\Gamma - A$, $\Gamma - \Sigma - M$ ($K - M - \Sigma$) directions has been corrected. The manifestation of the contributions of phonons from the $\Gamma - T - K$ direction to the second-order Raman spectra has been observed.

The paper is devoted to the study of second-order Raman spectra in semiconductor crystals with a structure of wurtzite. Multiphonon state spectra, Raman spectra in particular, are important since they allow one to estimate the density of vibration states in crystals and to obtain phonon dispersion along all the directions of the Brillouin zone, since phonons both from the zone center and its edges take part in a multiphonon scattering process.

Only phonons from the regions with high phonon state density per unit wave vector take part in the optical processes. Therefore, the information about the so-called critical points, which accord to a maximum of the phonon state density, is important. In particular, this is true for two-phonon states. The phonon frequency as a function of the wave vector shows an almost vanishing in one or several directions at the critical point of the dispersion branch. Therefore, the role of critical points is in that they allow one to estimate the contribution of certain regions of the Brillouin zone to the scattering process, without detailed specification of a complete function of the density of states.

We tried to compose a logical algorithm to study second-order Raman spectra, based on a combination of experimental data and a common method of a group-theoretic analysis of selection rules as well as on a determination of the points of zero slope based on the projective representation tools.

Zinc oxide crystals with the well-known wurtzite structure were chosen for testing the method of analysis of second-order Raman spectra in practice. The lattice symmetry of these crystals is characterized by a space group $P6_{3mc}$ (C_{6v}^4).

First, we constructed the irreducible representations $D_{\vec{k}}(h)$ ($h = (\vec{\alpha} + \vec{a}|r) \in G_{\vec{k}}$) of the wave vector groups $G_{\vec{k}}$, at the points of symmetry of the Brillouin zone of ZnO crystals. We used the method of construction of projective representations, presented in detail in [1, 2] and considered the points Γ, A, M, L, K, H, Δ, Σ, and T. It should be noted that, in the case of a study of states without considering the spin (integral spin), the elements which do not change the wave vectors or transform them into equivalent ones, are present in the point groups which describe the symmetry of equivalent directions for the groups of wave vectors of the main points of the Brillouin zone of wurtzite. That is why all elements of the quotient system $\omega_1(r_2, r_1)$ which is determined by the properties of a crystal space group are equal to unity for these points. It evidences for that these quotient systems coincide with the standard quotient systems of the class K_0, all elements of which are also equal to unity. Obtained representations of the wave vector groups coincide in general with those calculated in [3] by the method of loaded representations. We further took into account the time-inversion invariance, using the standard procedure of the Herring criterion. At some points, this led to an additional degeneracy. Namely, in the case b, complex conjugate non-equivalent representations are combined: $(A_1 + A_4)$, $(A_2 + A_3)$, $(A_5 + A_6)$ for point A, $(L_1 + L_4)$, $(L_2 + L_3)$ for point L, and $(H_1 + H_2)$ for point H, respectively.

To have information about whether an optical transition is allowed or forbidden, the total number of linearly independent nonzero matrix elements, which accords to the number of linearly independent invariants N_0 should be found. The mentioned invariants are contained in a direct product of irreducible

representations, by which the eigen wavefunctions of the initial and finite states as well as the excitation operators are transformed.

We were able to correctly apply the respective formulas from [1] for the determination of the number of linearly independent nonzero matrix elements after specifying to which case the irreducible representations of the groups of wave vectors, which accord to the main symmetry points of the Brillouin zone, can be attributed. We set $K^2 = 1$ in the formulas used, which corresponds to the states without the spin; $f = +1$, since we used dipole approximation. The latter means that the excitation operator is transformed as a product of coordinates, which shows a parity in relation to a time inversion.

Thus, the selection rules for overtone transitions as well as for the combinations for second-order Raman scattering and infrared absorption for ZnO crystals were found. The results of calculations are presented in Table 1.

In Table 1, $\chi_\rho(g)$ means characters of irreducible representations on which Raman-active components of the scattering tensor are transformed, or irreducible representations on which the components of a polar vector are transformed in the case of infrared absorption.

It should be noted that the Δ point has no symmetry elements which would transform the wave vector $\vec{k}_\Delta$ into the vector $-\vec{k}_\Delta$ in accordance with the quasi-momentum conservation law for the Raman process.

The results of calculations of the number of nonzero components of the momentum matrix elements p^α (N_1) as well as the number of components of the inverse effective mass tensor $1/m_{\alpha\beta}$ (N_2) are presented in Table 2.

To understand the complete second-order spectrum, we carried out the polarization measurements. The results of these measurements are presented in Figure.

The largest state density in the Brillouin zone of crystals with the wurtzite structure should be expected at the points along the $\Gamma - A$ direction, where there are the points of the highest symmetry. Previously [4, 5], we applied a method of construction of the dispersion curves of phonon states and the theory of large Jones zones for a partial interpretation of second-order Raman spectra in ZnO crystals in the $x(zz)y$ polarization, in which the intensity of a second-order spectrum is the highest in accordance with the selection rules. This is shown in Table 1.

Besides the dispersion curves of phonon states in the $\Gamma - A$ direction, refined by us [4, 5] we made use of the dispersion relations from [6, 7].

The behavior of phonon dispersion curves and the calculations carried out explain the nature of the second-order Raman spectrum in ZnO crystals. Namely, a line 209 cm^{-1} is an overtone of optical phonon Γ_5 (102 cm^{-1}) which originates from the acoustic mode of phonon states of the large Jones zone. A line 334 cm^{-1} is an overtone of point A at about 162 cm^{-1}. A line 541 cm^{-1} accords

Table 1. Selection rules for two-phonon processes for the symmetry points of the Brillouin zone for crystals with the wurtzite structure

$\chi_\rho(g)$	Overtones	Combinations
	Γ-point	
$\Gamma_1 \subset$ (Raman, infrared absorption)	$[\Gamma_1^2]$, $[\Gamma_4^2]$, $[\Gamma_5^2]$, $[\Gamma_6^2]$	$\Gamma_1 \times \Gamma_1$, $\Gamma_4 \times \Gamma_4$, $\Gamma_5 \times \Gamma_5, \Gamma_6 \times \Gamma_6$
$\Gamma_5 \subset$ (Raman)	$[\Gamma_5^2]$, $[\Gamma_6^2]$	$\Gamma_1 \times \Gamma_5$, $\Gamma_4 \times \Gamma_6$, $\Gamma_5 \times \Gamma_5$, $\Gamma_6 \times \Gamma_6$
$\Gamma_6 \subset$ (Raman, infrared absorption)	—	$\Gamma_1 \times \Gamma_6$, $\Gamma_4 \times \Gamma_5$, $\Gamma_5 \times \Gamma_6$
	A-point	
$\Gamma_1 \subset$ (Raman, infrared absorption)	$\left[(A_1+A_4)^2\right]$, $\left[(A_5+A_6)^2\right]$	$(A_1+A_4)\times(A_1+A_4)$, $(A_5+A_6)\times(A_5+A_6)$
$\Gamma_5 \subset$ (Raman)	$\left[(A_5+A_6)^2\right]$	$(A_1+A_4)\times(A_5+A_6)$, $(A_5+A_6)\times(A_5+A_6)$
$\Gamma_6 \subset$ (Raman, infrared absorption)	$\left[(A_5+A_6)^2\right]$	$(A_1+A_4)\times(A_5+A_6)$, $(A_5+A_6)\times(A_5+A_6)$
	M-point	
$\Gamma_1 \subset$ (Raman, infrared absorption)	$[M_1^2], [M_2^2]$, $[M_3^2], [M_4^2]$	$M_1 \times M_1, M_2 \times M_2$, $M_3 \times M_3, M_4 \times M_4$
$\Gamma_5 \subset$ (Raman)	$[M_1^2], [M_2^2]$, $[M_3^2], [M_4^2]$	$M_1 \times M_1, M_2 \times M_2$, $M_3 \times M_3$, $M_4 \times M_4$, $M_1 \times M_3$, $M_2 \times M_4$
$\Gamma_6 \subset$ (Raman, infrared absorption)	—	$M_1 \times M_2$, $M_1 \times M_4$, $M_2 \times M_3$, $M_3 \times M_4$
	L-point	
$\Gamma_1 \subset$ (Raman, infrared absorption)	$[(L_1+L_4)^2]$, $[(L_2+L_3)^2]$	$(L_1+L_4)\times(L_1+L_4)$, $(L_2+L_3)\times(L_2+L_3)$,
$\Gamma_5 \subset$ (Raman)	$[(L_1+L_4)^2]$, $[(L_2+L_3)^2]$	$(L_1+L_4)\times(L_1+L_4)$, $(L_1+L_4)\times(L_2+L_3)$, $(L_2+L_3)\times(L_2+L_3)$
$\Gamma_6 \subset$ (Raman, infrared absorption)	$[(L_1+L_4)^2]$, $[(L_2+L_3)^2]$	$(L_1+L_4)\times(L_1+L_4)$, $(L_1+L_4)\times(L_2+L_3)$, $(L_2+L_3)\times(L_2+L_3)$

Continuation

$\chi_\rho(g)$	Overtones	Combinations
	K-point	
$\Gamma_1 \subset$ (Raman, infrared absorption)	$([K_1^2])$, $([K_2^2])$, $([K_3^2])$	$K_1 \times K_1$, $K_2 \times K_2$, $K_3 \times K_3$
$\Gamma_5 \subset$ (Raman)	$([K_3^2])$	$K_1 \times K_3$, $K_2 \times K_3$, $K_3 \times K_3$
$\Gamma_6 \subset$ (Raman, infrared absorption)	—	$K_1 \times K_3$, $K_2 \times K_3$, $K_3 \times K_3$
	H-point	
$\Gamma_1 \subset$ (Raman, infrared absorption)	$([(H_1+H_2)^2])$, $([H_3^2])$	$(H_1+H_2) \times (H_1+H_2)$, $H_3 \times H_3$
$\Gamma_5 \subset$ (Raman)	—	$(H_1+H_2) \times H_3$, $H_3 \times H_3$
$\Gamma_6 \subset$ (Raman, infrared absorption)	$([H_3^2])$	$(H_1+H_2) \times H_3$, $H_3 \times H_3$
	Σ-point	
$\Gamma_1 \subset$ (Raman, infrared absorption)	$([\Sigma_1^2])$, $([\Sigma_2^2])$	$\Sigma_1 \times \Sigma_1, \Sigma_2 \times \Sigma_2$
$\Gamma_5 \subset$ (Raman)	$([\Sigma_1^2])$, $([\Sigma_2^2])$	$\Sigma_1 \times \Sigma_1, \Sigma_2 \times \Sigma_2$, $\Sigma_1 \times \Sigma_2$
$\Gamma_6 \subset$ (Raman, infrared absorption)	—	$\Sigma_1 \times \Sigma_1, \Sigma_2 \times \Sigma_2$, $\Sigma_1 \times \Sigma_2$
	T-point	
$\Gamma_1 \subset$ (Raman, infrared absorption)	$([T_1^2])$, $([T_2^2])$	$T_1 \times T_1$, $T_2 \times T_2$
$\Gamma_5 \subset$ (Raman)	$([T_1^2])$, $([T_2^2])$	$T_1 \times T_1$, $T_2 \times T_2 T_1 \times T_2$
$\Gamma_6 \subset$ (Raman, infrared absorption)	—	$T_1 \times T_1$, $T_2 \times T_2 T_1 \times T_2$

to an overtone of point Γ'. This band can also be attributed to phonons at about 270 cm^{-1}, which is between points Γ and M, as proposed in [6]. A band 1102 cm^{-1} recorded in spectra at different observation geometries should be attributed to overtones of point A at about 550 cm^{-1}. A band 1154 cm^{-1} typical of the spectra at all polarizations is the overtone of a longitudinal phonon Γ_{1LO}.

Besides the bands already described, the bands at frequencies 671, 792, and 986 cm^{-1} also draw attention in the Raman spectrum in the $x(zz)y$ polarization. The bands at 671 and 986 cm^{-1} were registered in all the polarizations studied. The band at 792 cm^{-1} is typical only for the Raman spectrum in the $x(zz)y$ polarization.

T a b l e 2. Number of nonzero p^α and $1/m_{\alpha\beta}$ components

N_1, N_2	Γ-point	
	Γ_1, Γ_2, Γ_3, Γ_4 (a_1 case)	Γ_5, Γ_6 (a_1 case)
N_1	0	0
N_2	2	3
	A-point	
	(A_1+A_4), (A_2+A_3) (b_1 case)	(A_5+A_6) (b_1 case)
	Diagonal matrix elements	
N_1	2	4
N_2	4	8
	Non-diagonal matrix elements	
N_1	1	1
N_2	2	5
	M-point	
	M_1, M_2, M_3, M_4 (a_1 case)	
N_1	0	
N_2	3	
	L-point	
	(L_1+L_4), (L_2+L_3) (b_1 case)	
	Diagonal matrix elements	
N_1	4	
N_2	8	
	Non-diagonal matrix elements	
N_1	1	
N_2	5	
	K-point	
	K_1, K_2(a_2 case)	K_3(a_2 case)
N_1	0	1
N_2	2	3
	H-point	
	(H_1+H_2), (H_1+H_2) (b_2 case)	
	Diagonal matrix elements	
N_1	2	
N_2	4	
	Non-diagonal matrix elements	
N_1	1	
N_2	2	
	H_3 (a_2 case)	
N_1	0	
N_2	3	
	Σ-point	
	Σ_1, Σ_2 (a_2 case)	
N_1	1	
N_2	3	
	T-point	
	T_1, T_2 (a_2 case)	
N_1	1	
N_2	3	

From the analysis of dispersion dependences, the band at 671 cm^{-1} should be attributed to two phonons in the $K - M - \Sigma$ direction at about 335 cm^{-1}. M is

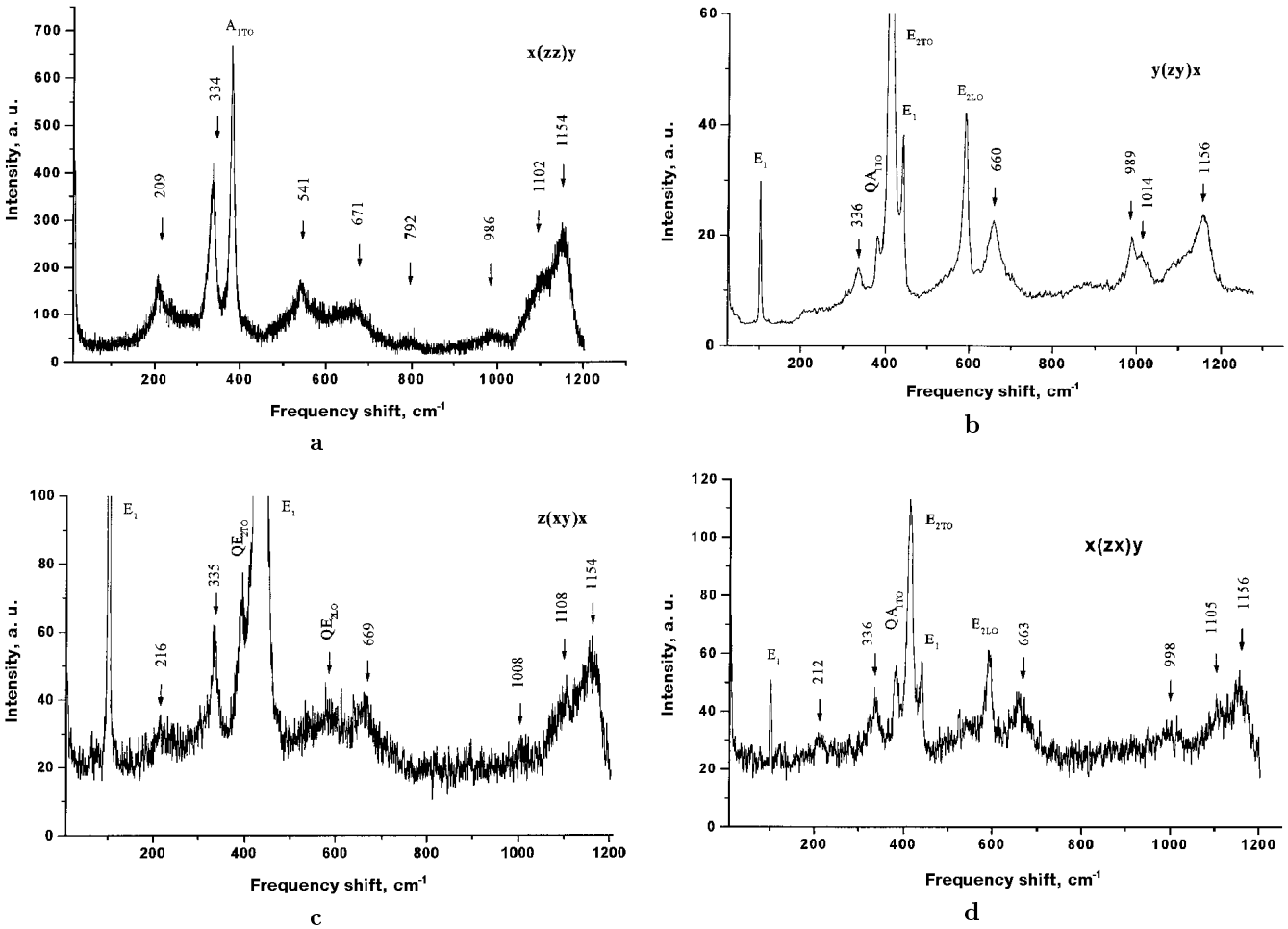

Raman spectrum of a ZnO single crystal at room temperature for different polarizations: $x(zz)y$ (a), $y(zy)x$ (b), $z(xy)x$ (c), and $x(zx)y$ (d)

a zero-slope point: $N_1 = 0$ for all the cases (see Table 2). The selection rules show (see Table 1) that the overtones of the M point are active in the (zz) and (xy) polarizations. Hence, if the mentioned band originates from the $K - M - \Sigma$ direction, the upper acoustic dispersion curve about point M should be higher in energy.

The energy position of a band at 792 cm^{-1} shows that the last belongs to the optical branch region. The manifestation of this band only in the $x(zz)y$ polarization shows that it is related rather to the overtone spectrum. However, the small intensity points out that it is not an overtone of the Γ point. From the examination of the trends of dispersion curves, a conclusion follows that the band at 792 cm^{-1} can be formed by the contributions of points from direction Γ — T – K at about 390 cm^{-1}. Point K is a zero-slope point for the cases K_1 and K_2 for all directions ($N_1 = 0$). The selection rules (see Table 1) confirm the polarization behavior of the overtones of point K. The highest activity should be observed in the (zz) polarization, which is confirmed by the experimentally measured second-order Raman spectra (Figure,a).

The band at about 986 cm^{-1} has a complicated structure which is mostly expressed in the $y(zy)x$ polarization, in which two components can be observed (Figure,b). The analysis of the energetic position of this band shows that this band is formed due to the combinations of the Γ point.

Therefore, it should be noted that the typical features of the considered two-phonon Raman spectra of ZnO crystals directly reflect the corresponding peculiarities of the density of two-phonon states in these crystals.

1. *Bir G.L., Pikus G.E.* Symmetry and Deformational Effects in Semiconductors. — Moscow: Nauka, 1972 (in Russian).

2. *Balchuk D.S., Bilyi M.M., Gryshchuk V.P. et al.* //Ukr. Fiz. Zh. — 1996. — **41**, N 2. — P. 146—155.

3. *Rashba E.I.* //Fiz. Tverd. Tela. — 1959. — **1**, Issue 3. — P. 407—421.

4. *Gerasimuk N.I., Gubanov V.A., Bilyi M.M.* //Proc. Intern. Conf. on Raman Spectr. XV, Pittsburh (USA), 1996. — P. 866—867.

5. *Berezovskaya N.I., Bilyi M.M., Gubanov V.O.* //Visn. Kyiv. Univ. Ser. Fiz.-Mat. Nauk. — 1999. — Issue 2. — P. 419—425.

6. *Calleja J.M., Cardona M.* //Phys. Rev. B. — 1977. — **16**, N 8. — P. 3753—3761.

7. *Hewat A.W.* //Solid State Communs. — 1970. — **8**, N 3. — P. 187—189.

Received 01.07.03.
Translated from Ukrainian by A.V. Sarikov

СПЕКТРОСКОПІЧНІ ДОСЛІДЖЕННЯ КРС ДРУГОГО ПОРЯДКУ ТА ВИЗНАЧЕННЯ ЕКСТРЕМАЛЬНИХ ЗНАЧЕНЬ ЩІЛЬНОСТІ ДВОФОНОННИХ СТАНІВ У КРИСТАЛАХ ZnO

В.О. Губанов, Н.І. Березовська

Р е з ю м е

Досліджено поляризовані спектри КРС другого порядку в кристалах ZnO та проведено їх інтерпретацію на основі теоретико-групового аналізу правил добору та визначення точок нульового нахилу дисперсійних кривих фононних станів, що отримані за єдиною методикою із застосуванням апарату проективних представлень. Розглянуто точки Γ, A, M, L, K, H, Δ, Σ, T зони Бріллюена. Уточнено хід дисперсійних кривих фононних станів в напрямках Γ — A, Γ — Σ — M (K — M — Σ). Зареєстровано прояв внесків фононів, які відповідають точкам з напрямку Γ — T — K, в спектр КРС другого порядку.